J|A|C|S
ARTICLES
Published on Web 01/31/2006

NMR Chemical Shift Powder Pattern Recoupling at High Spinning Speed and Theoretical Tensor Evaluation Applied to Silk Fibroin

Raiker Witter,*,† Ulrich Sternberg,† and Anne S. Ulrich†,‡

Contribution from the Forschungszentrum Karlsruhe, IBG, POB 3640, 76021 Karlsruhe, Germany, and University of Karlsruhe, IOC, Fritz-Haber-Weg 6, 76131 Karlsruhe, Germany

Received April 11, 2005; E-mail: Raiker.Witter@ibg.fzk.de

Abstract: The NMR pulse sequence RAI (recoupling of anisotropy information) has been improved to obtain powder patterns at high MAS spinning speeds. The 2D iso-aniso experiment displays the static chemical shift spectra on the indirect dimension and the MAS spectra on the direct dimension; hence overlapping chemical shift tensor patterns can be well resolved. This efficient technique is applicable to compounds containing ^{13}C sp^3 (C_α, C_β) and sp^2 (C═O) sites with higher chemical shift (CS) anisotropy (CSA), and the reliability of the method was tested here on the ^{13}C chemical shift tensors of polycrystalline glycine, alanine, and serine. Subsequently, the same experiment was applied to the native silk protein fibroin from *Bombyx mori*, which consists mainly of these three amino acids. Molecular dynamics (MD) simulations of the silk II crystal structure of Takahashi et al. (Takahashi et al. *Int. J. Biol. Macromol.* **1999**, *24*, 127−138) were carried out to study the influence of motions on the chemical shift tensors. The ^{13}C chemical shift tensors were calculated using the bond polarization theory BPT on 200 structures created by an MD simulation. Very good agreement of the theoretical chemical shift anisotropy values with the experimental NMR results was obtained. The tensor orientations in the protein structure could thus be reliably derived.

Introduction

Chemical shift anisotropy (CSA) parameters can be extracted by a variety of NMR techniques.[1−9] Here, we present an improved MAS pulse sequence that is suitable for high spinning speeds up to 15 kHz. It is based on the 2D iso-aniso experiment originally devised by Tycko,[6] which was developed further by Witter[7] and named RAI (recoupling of anisotropy information). The newly improved sequence has remarkable advantages: (i) it provides better resolution in the isotropic dimension due to high MAS speeds, (ii) recoupling is achieved with robust echo pulses over an odd number of rotor periods, and hence (iii) it can be conveniently scaled to address large anisotropies. Furthermore, (iv) finite pulse lengths are taken into account to avoid artifacts; (v) shearing (isotropic shift and offset are scaled) can be avoided by choosing appropriate echo intervals and pulse timings.

To demonstrate its potential, RAI is applied here to *Bombyx mori* silk fibroin, a protein that forms heterogeneous semicrystalline fibers. So far, diffraction investigations of those materials only yielded preliminary structures; hence a refined analysis based on NMR chemical shifts promises further insight into the connection between molecular structure and material properties. In a recent application of cellulose, we have shown that the experimental isotropic chemical shifts can be used as valuable constraints to refine existing crystal structures (Sternberg et al.[10]). As a general strategy we compare the experimental ^{13}C chemical shifts tensor components (extracted from the RAI spectrum) with a molecular dynamics simulation of motional chemical shift tensor averages which starts from the available crystal coordinates.[11,12] We are thus able to provide complete data on the three-dimensional orientation of each individual chemical shift tensor. This information is a prerequisite for all further solid-state NMR investigations on oriented samples or any tensor correlation experiments (see, e.g., Ashida et al.[13]).

The present investigation of silk demonstrates how the new combination of an improved RAI experiment and an MD-based data analysis can provide insight into structural details of native (unlabeled) fibrous proteins and how the NMR parameters of all carbon sites can be derived. The ultimate aim of this investigation is to pave the way for a general structure refinement of proteins using NMR chemical shifts, which should be applicable to crystalline, semicrystalline, and membranous

† Forschungszentrum Karlsruhe.
‡ University of Karlsruhe.

(1) Antzutkin, O. N.; Shekar, S. C.; Levitt, M. H. *J. Magn. Reson.* **1995**, *115*, 7.
(2) Dixon, W. T. *J. Chem. Phys.* **1982**, *77*, 1800.
(3) Hu, J. Z.; Wang, W.; Liu, F.; Solum, M. S.; Alderman, D. W.; Pugmire, R. J.; Grant, D. M. *J. Magn. Reson.* **1995**, *113*, 210.
(4) Alderman, D. W.; McGeorge, G.; Hu, J. Z.; Pugmire, R. J.; Grant, D. M. *Mol. Phys.* **1998**, *95*, 1113.
(5) Liu, S.-F.; Mao, J. D.; Schmidt-Rohr, K. *J. Magn. Reson.* **2002**, *155*, 15.
(6) Tycko, R.; Dabbagh, G.; Mirau, P. A. *J. Magn. Reson.* **1989**, *85*, 265.
(7) Witter, R.; Hesse, St.; Sternberg, U. *J. Magn. Reson.* **2002**, *161*, 35.
(8) Chan, J. C. C.; Tycko, R. *J. Chem. Phys.* **2003**, *118*, 8378.
(9) Hodgkinson, P.; Emsley, L. *J. Chem. Phys.* **1997**, *107*, 4808.
(10) Sternberg, U.; Koch, F.-Th.; Prieβ, W.; Witter, R. *Cellulose* **2003**, *10*, 189.
(11) Koch, F.-T.; Prieβ, W.; Witter, R.; Sternberg, U. *Macromol. Chem Phys.* **2000**, *201*, 1930.
(12) Sternberg, U.; Witter, R.; Ulrich, A. S. *Ann. Rep. NMR Spectrosc.* **2004**, *52*, 54.
(13) Ashida, J.; Ohgo, K.; Asakura, T. *J. Phys. Chem. B* **2002**, *106*, 9434.

10.1021/ja051730f CCC: $33.50

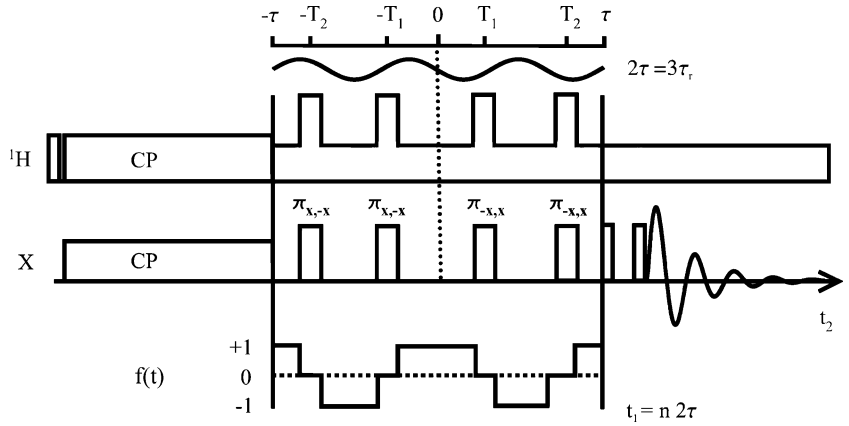

Figure 1. Four-pulse RAI sequence for recoupling the CSA powder pattern over three rotor cycles τ_r. First, equilibrium ^{1}H magnetization is brought into the $x-y$ plane and transferred via cross polarization to ^{13}C (X). Then, during the indirect evolution time t_1, a sequence of π-pulses on the X-channel recouples the chemical shift anisotropy powder pattern. After a z-filter the, direct dimension FID, t_2, is recorded under pure MAS evolution. Heteronuclear interactions with the ^{1}H nuclei are decoupled by CW irradiation as well as high power pulses.

samples. To take advantage of the wealth of information that is contained in the chemical shift tensor data, we have verified here that our methods can indeed be reliably applied to proteins.

NMR Experiment

The 2D RAI experiment recouples the chemical shift anisotropy to obtain powder patterns in the indirect dimension. This is achieved by properly rotor-synchronized π-pulses during $N = 3$ and 5 ($\tau = \tau_r N/2$) rotor cycles, taking finite pulse lengths into account. The method is thus applicable to large anisotropies and high MAS spinning speeds. The artifacts associated with the earlier experiment of Tycko et al.[6] are drastically reduced. The pulse sequence is shown in Figure 1.

In our system the time-dependent NMR energy operator for ^{13}C detection can be expressed by[14]

$$H(t) = \hbar \sum_i (I_z^{13_{Ci}} \omega_{cs}^{\ i}(t) + \sum_j I_z^{13_{Ci}} I_z^{1_{Hj}} \omega_D^{\ ij}(t)). \quad (1)$$

The chemical shift and heteronuclear coupling frequencies, $\omega_{cs}(t)$ and $\omega_d(t)$, under MAS conditions (spinning frequency ω_r) have the general form

$$\omega(t) = \Delta\omega + C_1 \cos(\omega_r t) + C_2 \cos(2\omega_r t) + S_1 \sin(\omega_r t) + S_2 \sin(2\omega_r t) \quad (2)$$

In the static case, where $t = 0$, only the coefficients $C_1(\Omega)$ and $C_2(\Omega)$ are left. The angles $\Omega = (\alpha,\beta,\gamma)$ represent the orientation of the chemical shift tensor with respect to the molecular frame. To recouple undistorted powder patterns, these coefficients have to be reintroduced with equal weighting, $\chi(C_1 + C_2)$. The asymmetric sine contributions can be suppressed by symmetric pulse sequences, as illustrated in Figure 1. The pulse timings are evaluated by fulfilling the following condition

$$\int_0^\tau f(t) \cos(\omega_r t)\, dt = \int_0^\tau f(t) \cos(2\omega_r t)\, dt \quad (3)$$

where $f(t)$ is a kind of step function having the value 0 during the action of the pulses and otherwise alternating between -1 and $+1$, according to the spin flipping of the π-pulses. The coefficients C_1 and C_2 are scaled by a constant, χ, which is the scaling factor of the width of the powder pattern. It is

$$\chi = \frac{1}{\tau}\int_0^\tau f(t) \cos(\omega_r t)\, dt \quad (4)$$

The constant frequency part $\Delta\omega$ is multiplied by

$$\xi = \frac{1}{\tau}\int_0^\tau f(t)\, dt \quad (5)$$

Equation 3 always has to be fulfilled. The next equation, eq 4, is useful because the width of the powder pattern can be scaled such as to fit within the experimental accessible spectral window. Equation 5 defines the shearing constant ξ. It is advisable to avoid shearing ($\xi = 0$).

For a four-pulse sequence the nonlinear eq 3 has to be solved. The functional behavior of the solution for the case of $N = 5$ is shown in Figure 2. In a general formulation it is very useful to approximate the solutions of pulse timings, T_i, scaling factor, χ, and shearing constant, ξ, as polynomial functions of the relative pulse timing (T_1/τ):

$$\left(\frac{T_i}{\tau}\right) = \sum_k a_k \left(\frac{T_1}{\tau}\right)^k$$

$$\chi = \sum_k b_k \left(\frac{T_1}{\tau}\right)^k$$

$$\xi = \sum_k c_k \left(\frac{T_1}{\tau}\right)^k. \quad (6)$$

Appropriate intervals are selected where the solutions of the equations display no discontinuities. As an example, the coefficients for the four-pulse sequence using five rotor periods for recoupling are listed in Table 1. For the four-pulse sequence with $\tau_\pi = 6$ μs, $\tau = 2.5\tau_r$ ($w_r = 15$ kHz), we can choose the timing for the third pulse as $T_1 = 0.1115\tau$, then it follows from eqs 6 that $T_2 = 0.3615\tau$, $\chi = +0.0711$, and $\xi = 0$ (no shearing). For the four-pulse sequence with $N = 3$, $\tau_\pi = 6$ μs, $\tau = 1.5\tau_r$ ($\tau_r = 10$ kHz) we obtain by solving the eqs 3−5: $T_1 = 0.1484\tau$, $T_2 = 0.3984\tau$, $\chi = -0.1256$, and $\xi = 0$.

The RAI sequence with finite pulse lengths provides undistorted and well resolved static powder spectra with a high signal-to-noise ratio. If the correct phase cycle is applied (see Figure 1) B_1 field inhomogeneities are suppressed. In Figure 3 the influences of the finite pulse length and B_1 field inhomogeneities are demonstrated by numerical SIMPSON[15] simulations. A π-pulse length of 6.0 μs for the carbon channel and a field inhomogeneity of -10% have negligible influence on the powder pattern line shape. The distortions at the edges of the spectral window can be considered as a measure of inhomogeneity. In our experiments with rotors of a 4 mm diameter, any distortions are most significantly reduced by carefully adjusting pulse lengths. In

(14) Schmidt-Rohr, K.; Spiess, H. W. *Multidimensional Solid-State NMR and Polymers*; Academic Press: San Diego, CA, 1996.

(15) Bak, M.; Rasmussen, J. T.; Nielsen, N. C. *J. Magn. Reson.* **2000**, *26*, 1.

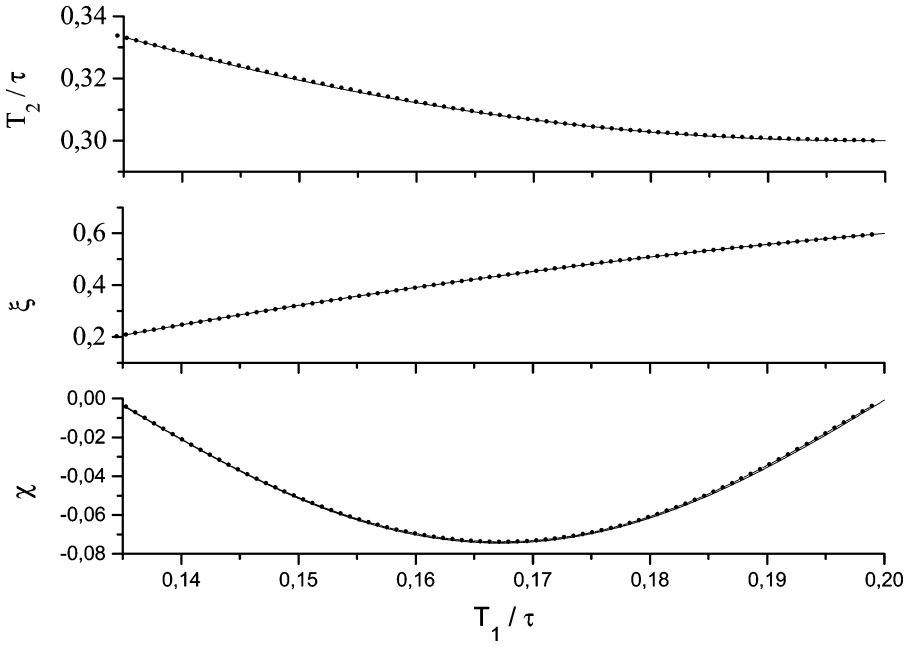

Figure 2. Functional dependence on the relative pulse timing T_1/τ of the pulse timings T_2, the shearing constant ξ, and the scaling factor χ of the four-pulse RAI sequence for recoupling over 5 rotor periods. The dependence is given for the continuous interval between 0.135 and 0.2. A finite π-pulse length of 6.0 μs is introduced.

Table 1. Coefficients of the Polynomial Approximation of the Four-pulse RAI Sequence $(T_1/\tau) \in (0.135, 0.2)$; See Eq 6

Four-Pulse Sequence ($5\tau_r/\tau_\pi$ 6 μs/15 kHz)			
k	a_k of T_2	b_k of χ	c_k of ξ
0	+0.627 32	−7.39006	−1.509 30
1	−3.2975	+201.6901	+17.1900
2	+8.309	−1967.383	−33.236
3	0	+8150.37	0
4	0	−12 159.6	0
R		>0.998	
SD		$<10^{-4}$	

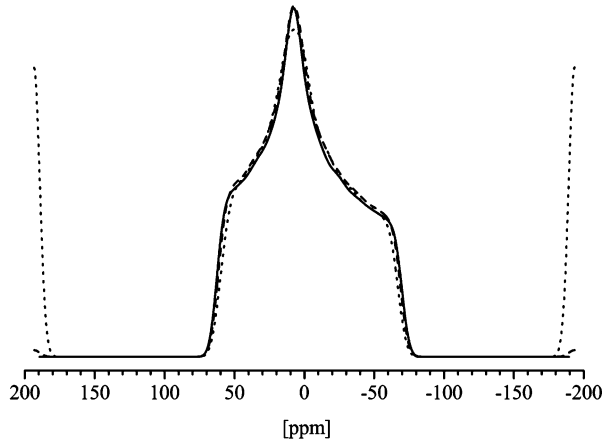

Figure 3. SIMPSON[15] simulation of the RAI sequence of a ^{13}C alanine carbonyl chemical shift powder pattern: $T_1 = 0.1115\tau$, $T_2 = 0.3615\tau$, $\chi = +0.0711$ ($\xi = 0$, $\tau = {}^5/_2\tau_r$, and $\omega_\tau = 15$ kHz), (—) ideal pulses, (· · ·) real π -pulses of 6.0 μs duration, (- -) 6.0 μs pulses with −10% rf field deviation is similar to a B_1 field of 90%.

addition to the CSA, also the heteronuclear couplings are reintroduced by the RAI sequence, and the effect of the protons vanishes only when ^{1}H-decoupling is applied. During the pulses on the X-channel, high power radiation should thus be applied on ^{1}H, for which 2π-pulse lengths of 6.0−8.0 μs are sufficient.[5,16]

Applications

The NMR experiments were performed on a Bruker[17] Avance 500 spectrometer with two 1 kW transmitters. Rotors with a diameter of 4 mm were conveniently spun up to 15 kHz with a Bruker MAS unit. No special triggering of the rotor-synchronized pulses is necessary if more than four scans for averaging are used. The carbon π-pulse length was adjusted to be 6.0 μs. For the high power ^{1}H pulse decoupling a 2π-pulse length of 6.0 μs was used. That way, the $B_{1,H}$ field strength satisfied the relation $\omega_{1,H}/\omega_{1,C} \approx 2$ which is sufficient for suppression of ^{13}C−^{1}H heteronuclear interaction.[16] This condition ensured satisfactory powder patterns. The four-pulse sequence with zero shearing at 12.5 kHz was applied, with the following pulse timings: $T_1 = 0.148\tau$, $T_2 = 0.398\tau$, $\chi = -0.1225$ ($\xi = 0$, $\tau = 3/2\tau$). For cross polarization at high spinning speed we applied a standard RAMP[18] sequence for better efficiency.

First, the improved RAI sequence was tested on the three polycrystalline amino acids glycine, alanine, and serine, as summarized in Table 2. For such model compounds the ^{13}C spin density per amino acid and sample volume are higher than those in a protein, and they are readily measured. For example, it takes 15 min to obtain a high signal-to-noise 2D RAI spectrum of glycine. Other precise chemical shift tensor values are available from the literature[19] which can be compared to our results.

The CSA analysis was performed using the powder pattern fit routine DMfit.[20] The standard deviation from earlier published experimental work[15] was found to be 4.5 ppm. It turned out that the deviations of δ_{11} and δ_{33} are around 5.5 ppm, but for the δ_{22} component it is much smaller at 1.4 ppm. This systematic

(16) Ishii, Y.; Ashida, J.; Terao, T. *Chem. Phys. Lett.* **1995**, *246*, 439.
(17) BRUKER (Karlsruhe, Germany).
(18) Wu, X.; Zilm, K. W. *J. Magn. Reson. A* **1993**, *104*, 154. Peersen, O. B.; Wu, X.; Kustanovich, I.; Smith, S. O. *J. Magn. Reson. A* **1993**, *104*, 334.
(19) Ye, C.; Fu, R.; Hu, J.; Hou, L.; Ding, S. *Magn. Res. Chem*, **1993**, *31*, 699.
(20) Massiot, D.; Fayon, F.; Capron, M.; King, I.; Calve, S. L.; Alonso, B.; Durand, J. O.; Bujoli, B.; Gan, Z.; Hoatson, G. *Magn. Res. Chem.* **2002**, *40*, 70.

Table 2. ^{13}C CSA Values of Polycrystalline Amino Acids Glycine and Alanine Measured with the RAI Sequence and Corresponding Single-Crystal Results;[19] the Calculated Standard Deviation between Both Techniques is 4.5 ppm

	RAI experiment				single-crystal investigations (Ye et al.[19])		
carbon	δ_{iso}	δ_{11}	δ_{22}	δ_{33}	δ_{11}	δ_{22}	δ_{33}
Gly C_α	43.5	56(2)	47.0 (0.5)	27(2)	61(3)	46(1)	24(5)
Gly CO	176.2	250(2)	179.5(0.5)	99(2)	246(1)	179(1)	106(1)
Ala C_α	49.9	56(2)	55.5(0.5)	27(2)	63(1)	56(1)	30(3)
Ala C_β	18.6	27(2)	18.5(0.5)	10(2)	31(2)	19(2)	7(2)
Ala CO	175.7	243(2)	183.5(0.5)	100(2)	239(4)	184(3)	106(1)
Ser C_α	54.5	62(2)	56.5(0.5)	45(2)	69(3)	59(1)	39(1)
Ser C_β	61.7	82(2)	66.5(0.5)	37(2)	87(3)	66(2)	35(2)
Ser CO	174.1	245(2)	172.0(0.5)	105(2)	238(4)	175(3)	113(3)

error can be understood as a consequence of the B_1 field inhomogeneity; see Figure 3. The powder pattern is broadened, and it is indeed easier to simulate a peak of a function than to accurately determine its broadened edges.

Next, the RAI sequence was applied to a *Bombyx mori* silk fibroin to extract the CSA parameters from this native protein. Spider and silkworm silks are fibrous proteins with numerous actual and potential applications. These polymeric biomaterials are rather heterogeneous and partially amorphous; hence they cannot be sufficiently characterized using diffraction methods only. Silk fibers are therefore extensively studied using NMR methods (for review see for instance Zhao et al.[21]). In this work the semicrystalline domains of degummed silk fibroin were studied, consisting mainly of β-sheets (Silk II structure, see ref 21). The primary structure of this protein is built up mainly of (-Gly-Ala-Gly-Ala-Gly-Ser-)-hexamers or -octamers, with a low content of tyrosine. From diffraction studies of the semicrystalline silk Cp-fraction (chymotrypsin cleaved precipitate, Takahashi et al.[22]) it was concluded that the unit cell of these domains contains two antipolar antiparallel β-sheet structures with different orientations, as illustrated in Figure 4. Because of the relatively low resolution of X-ray fiber diffraction studies, the quest for the proper Silk II structure has not been settled yet. Alternative structural models were published by Fossey et al.[23] and Asakura et al.[24] The 1D ^{13}C NMR spectrum obtained in our work resembles in nearly all features the pattern published by Kameda and Asakura[25] and Zhao and Asakura;[21] hence we assigned our resonances according to those results. The ^{13}C chemical shift anisotropy of the glycine and alanine residues could be determined from 1D slices of the 2D pattern of the RAI spectrum given in Figure 5. For the small serine and tyrosine content, the signal-to-noise ratio was not sufficient. The results are compiled in Table 3 together with the experimental and theoretical values from other authors. The ^{13}C chemical shift anisotropies for fibroin from *Bombyx mori* had been measured for the carbonyl carbons of alanine and glycine by Demura et al.[26] The CSA values for the corresponding C_α and C_β sites are determined for the first time here in this work. Anisotropy data for other polypeptides can be found in a paper of Wei et al.,[27] who performed 2D PASS measurements for commercially available polypeptides and dipeptides. We also compare our measurements to the carbonyl tensor values of glycine reported for a model amyloid fibril by Costa et al.[28] Values from a poly-L-Ala-sheet are also included in Table 3, because in this case the main difference is the presence of glycine residues adjacent to alanine. Zhou et al.[29] have compared DFT chemical shift calculations for several *B. mori* fibroin models with NMR experiments to verify the Silk I or II structures.

MD Simulation of Chemical Shift Spectra in Crystalline Silk Fibroin

For the MD simulations of crystalline fibroin, we used The COSMOS force field[30] and the ^{13}C chemical shift tensors are calculated using the bond polarization theory (BPT).[31−33] The general features of this method are briefly outlined below. The chemical shift tensor is defined by[34]

$$\hat{\delta} = \hat{\sigma}_{\mathrm{ref}} - \hat{\sigma}_N \tag{7}$$

and it can be expressed as a sum of one-electron operators. Within the BPT approach[31,32] the chemical shift tensor is given by

$$\langle \Psi_0 | \hat{\delta}_{\alpha\beta} | \Psi_0 \rangle = \sum_i^{i\in A} \sum_{\alpha\alpha'\beta\beta'} D^i_{\alpha\alpha'} D^i_{\beta\beta'} (n_i \delta_i^{\alpha'\beta'} + n_i^2 A(\delta)_i^{\alpha'\beta'} [\langle \chi_A{}^i | \hat{V} | \chi_A^i \rangle - \langle \chi_B{}^i | \hat{V} | \chi_B^i \rangle]), \tag{8}$$

where the matrix elements $D_{\alpha\alpha'}$ describe the coordinate transformation from the bond orbital frame to the reference frame. The first sum runs over all bond contributions of atom *A*. The bond polarization matrix elements are given by

$$\langle \chi_\lambda | \hat{V} | \chi_\lambda \rangle = \sum_x^{\text{charges}} \sum_k h_k^2 \int \phi_k^\lambda(r) \frac{Q_x}{|\vec{R}_x - \vec{r}|} \phi_k^\lambda(r)\, \mathrm{d}r^3 \tag{9}$$

with the charges Q_x at position $\vec{R}_x$, the Slater type orbitals,[35] $\phi_k^\lambda(r)$, and the bond orbital coefficients h_k. The first sum runs over all polarizing atomic charges. The polarization parameters $\delta_i^{\alpha\beta}$ and $A(\delta)_i^{\alpha\beta}$ were obtained by a calibration procedure by Sternberg et al.[32,34] To that aim collection of crystal structures and single-crystal ^{13}C chemical shift measurements[36,37] had been used to establish a set of linear equations, and ab initio results were also utilized. The correlation coefficient for the parameter calibration was $R = 0.994$ with a standard deviation of SD = 7.2 ppm. Once the parameters $\delta_i^{\alpha\beta}$ and $A(\delta)_i^{\alpha\beta}$ have been determined, only the matrix elements $\langle \chi_A^i | \hat{V} | \chi_A^i \rangle$ as well as $\langle \chi_B^i | \hat{V} | \chi_B^i \rangle$ and the occupation numbers[38] n_i have to be calculated. They are all expressed analytically; hence the high calculation efficiency of the BPT formula is obvious. In eq 8,

(21) Zhao, C.; Asakura, T. *Prog. Nucl. Magn. Reson. Spectrosc.* **2002**, *39*, 301.
(22) Takahashi, Y.; Gekoh, M.; Yuzuriha, K. *Int. J. Biol. Macromol.* **1999**, *24*, 127.
(23) Fossey, S. A.; Nemethy, G.; Gibson, K. D.; Scheraga, H. A. *Biopolymers* **1991**, *31*, 1529.
(24) Asakura, T.; Demura, M.; Date, T.; Miyahita, N. *Biopolymers* **1997**, *41*, 193.
(25) Kameda, T.; Asakura, T. *Ann. Rep. NMR Spectrosc.* **2002**, *46*, 101.
(26) Demura, M.; Minami, M.; Asakura, T.; Cross, T. *J. Am. Chem. Soc.* **1998**, *120*, 1300.
(27) Wei, Y.; Lee, D. K.; Ramamoorthy, A. *J. Am. Chem. Soc.* **2001**, *123*, 6118.
(28) Costa, P. R.; Kocisko, D. A.; Sun, B. Q.; Lansbury, P. T.; Griffin, R. G. *J. Am. Chem. Soc.* **1997**, *119*, 10487.
(29) Zhou, P.; Li, G.; Shao, Z.; Pan, X.; Yu, T. *J. Phys. Chem.* **2001**, *105*, 12469.
(30) Sternberg, U.; Koch, F. T.; Losso, P. *www.cosmos-software.de.* **2005**.
(31) Sternberg, U. *J. Mol. Phys.* **1988**, *63*, 249.
(32) Sternberg, U.; Priess, W. *J. Magn. Reson.* **1997**, *125*, 8.
(33) Prieβ, W.; Sternberg, U. *THEOCHEM* **2001**, *544*, 181.
(34) Mason, J. *Sol. Stat. Nucl. Magn. Reson.* **1993**, *2*, 285.
(35) Slater, J. C. *Phys. Rev.* **1930**, *36*, 57.
(36) Veeman, W. S. *Prog. NMR Spectrosc.* **1984**, *20*, 193.
(37) Sherwood, M. H.; Alderman, D. W.; Grant, M. G. *J. Magn. Reson.* **1989**, *84*, 466.

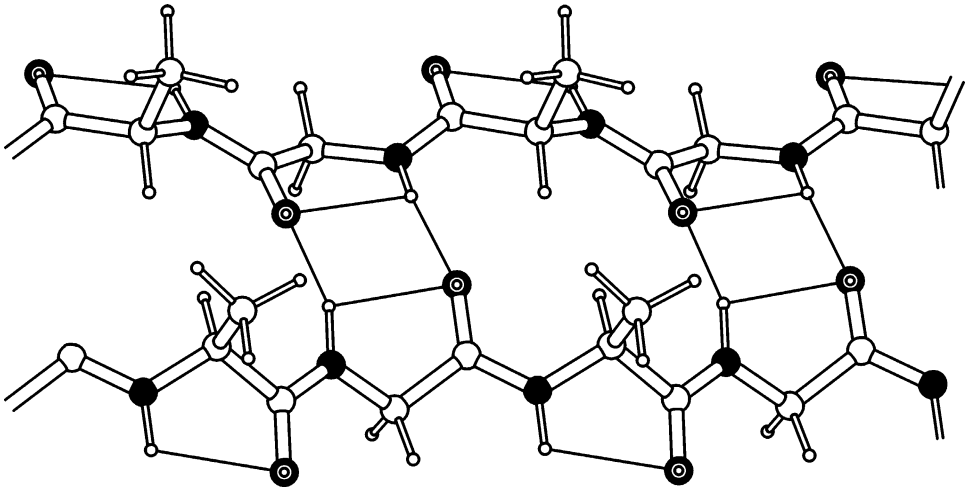

Figure 4. *Bombyx mori* Silk II model of Takahashi et al.,[22] consisting of two antipolar-antiparallel β-sheet structures ([Gly-Ala]$_n$) with different orientations.

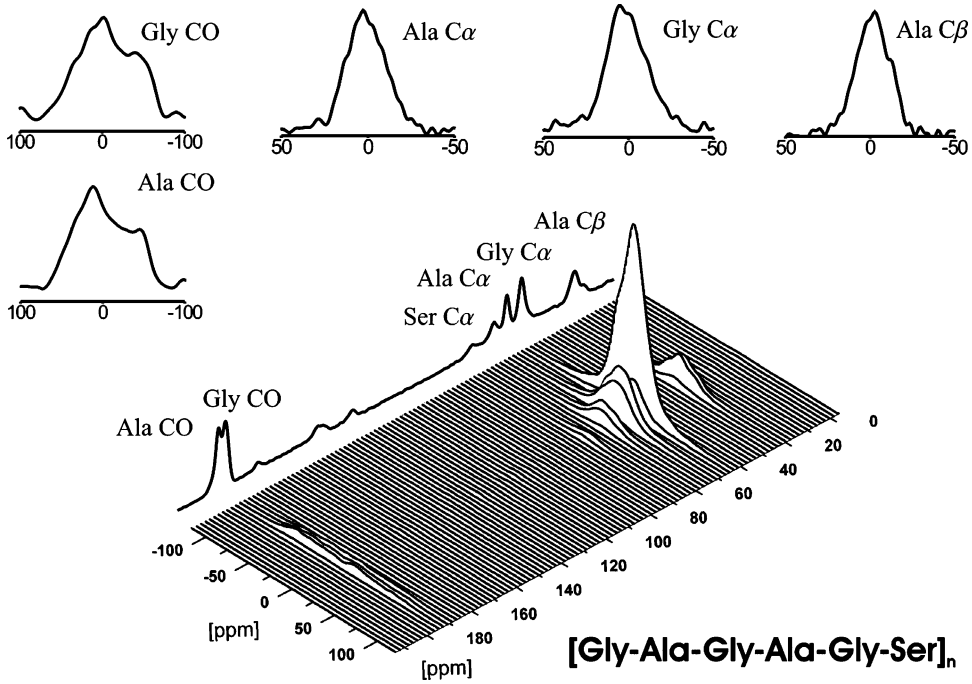

Figure 5. 2D RAI spectrum and six extracted powder patterns of silk fibroin. The spectrum was obtained at a 12.5 kHz MAS spinning frequency in roughly 14 h (48 t_1 data points, 1024 scans, 1 s repetition time). The overlapping CS tensors patterns, especially Gly C═O and Ala C═O, are well resolved.

there are two sums: the first runs over all bond contributions of the atom under consideration, and the second runs over all polarizing atomic charges of $\hat{V}$. Hence, if the atomic charges are known, the computational cost for a chemical shift calculation is proportional to N_A, the number of atoms. The charge calculation is also performed within the BPT approach.[39]

$$Q_A = \sum_i^{i\in A} (n_i q_i + n_i^2 A(q)_i [\langle \chi_A^i | \hat{V}_2 | \chi_A^i \rangle - \langle \chi_B^i | \hat{V}_2 | \chi_B^i \rangle]) \quad (10)$$

Given these charge equations, the charges Q_A have to be estimated from the charges Q_x

$$Q_A = \sum_i^{i\in A} \left(n_i q_i + n_i^2 A(q)_i \sum_x^{\text{charges}} \left[\left\langle \chi_A^i \left| \frac{Q_x}{|\vec{R}_x - \vec{r}|} \right| \chi_A^i \right\rangle - \left\langle \chi_B^i \left| \frac{Q_x}{|\vec{R}_x - \vec{r}|} \right| \chi_B^i \right\rangle \right] \right) \quad (11)$$

The parameters q_i and $A(q)_i$ had been calibrated on atomic charges from a natural population analysis (NAP) of a set of 175 molecular structures consisting of H, C, N, O, F, Si, P, S, Cl, and Zn atoms.[40] The computational time for setting up all charge equations is proportional to N_A^2. To calculate the charges, this set of linear equations has to be solved, for which the number of operations is proportional to N_A^3.

The information content of conventional NMR spectra is an average over a sample volume of about 100 mm^3 and a time scale of microseconds. Therefore, statistical methods are crucial for NMR parameter simulations. In this work the ^{13}C chemical shift tensor averaging was achieved by molecular dynamics simulation, using a modified leapfrog scheme to generate trajectories within the constant-NVT ensemble.[41] For the

(38) O'Keefe, M.; Brese, N. E. *J. Am. Chem. Soc.* **1991**, *113*, 3226.
(39) Koch, F. T.; Möllhoff, M.; Sternberg, U. *J. Comput. Chem.* **1994**, *15*, 524.
(40) Witter, R. *Three Dimensional Structure Elucidation with the COSMOS-NMR Force Field*, Ph.D. Thesis, Physikalisch-Astronomischen Fakultät der Friedrich-Schiller-Universität Jena. www.dissertation.de, 2003.

Table 3. ^{13}C CSA Values of *B. mori* Silk Fibroin Obtained with the RAI Experiment, Compared with Results from the Literature[a]

		RAI[b]	Zhao[21]	Demura[26]	Wei[27]	Costa[28]	Zhou[29]	MD[b]	static[b]
Ala C_β	δ_{iso}	20.2	20.2					21(4)	22(4)
	δ_{11}	39(2)						31(8)	32(8)
	δ_{22}	20(1)						30(8)	29(8)
	δ_{33}	1(2)						3(8)	3(8)
Val C_β	δ_{iso}	29.9							
Tyr C_β	δ_{iso}	35.5							
Gly C_α	δ_{iso}	43.2	43.1					36(4)	37(4)
	δ_{11}	61(2)						62(8)	62(8)
	δ_{22}	47(1)						43(8)	41(8)
	δ_{33}	21(2)						10(8)	9(8)
Ala C_α	δ_{iso}	49.4	49.4		48.9			48(4)	51(4)
	δ_{11}	71(2)			64.6			67(8)	66(8)
	δ_{22}	51(1)			49.7			52(8)	52(8)
	δ_{33}	26(2)			32.4			32(8)	34(8)
Ser C_α (TyrC_a)	δ_{iso}	55.2	55.4						
Val C_β	δ_{iso}	60.9							
Ser C_β	δ_{iso}	64.7	63.6						
Tyr C_ϵ	δ_{iso}	115.8							
Tyr C_γ	δ_{iso}	128.4							
Tyr C_δ	δ_{iso}	130.4							
Tyr C_ξ	δ_{iso}	155.9							
Gly CO	δ_{iso}	169.6	169.5	174.3		169.3	167.4	159(4)	175(4)
	δ_{11}	232(2)		245(5)		245	246.8	231(8)	249(8)
	δ_{22}	178(1)		179(5)		176	164.3	175(8)	169(8)
	δ_{33}	99(2)		99(5)		87	91.0	93(8)	108(8)
AlaCO (TyrCO)	δ_{iso}	172.6	172.3	174.7	173.1		172.5	165(4)	164(4)
	δ_{11}	232(2)		242(5)	248.3		249.2	236(8)	239(8)
	δ_{22}	186(1)		186(5)	180.1		177.6	173(8)	157(8)
	δ_{33}	99(2)		96(5)	90.9		90.8	105(8)	95(8)
Ser CO	δ_{iso}	173.1	172.3						

[a] In Zhao et al.,[29] ^{13}C CP/MAS NMR chemical shifts of the amino acid residues of *B. mori* fibroin (Silk II) are represented. In the work of Demura et al.,[26] experimental solid state ^{13}C enriched power patterns were fitted without considering ^{15}N−^{13}C coupling. The ^{13}C tensor values of Wei et al.[27] correspond to experimental data of poly-L-Ala. Costa et al.[28] determined glycine carbonyl tensors of model amyloid fibrils (results on GG-HCl represented here). In the paper of Zhou et al.,[29] DFT chemical shift calculations for the model of Fossey et al.[23] considering H-bonds are listed. [b]Results of this work. We used the convention $|\delta_{33} - \delta_{iso}| \geq |\delta_{11} - \delta_{iso}| \geq |\delta_{22} - \delta_{iso}|$.

potential energy, we used the COSMOS force field,[42] with the common contributions

$$U^{total} = U^{bond} + U^{nonbond} \quad (12)$$

for the bonded and nonbonded energies. The bonded interactions include terms which describe the potential energy for bond stretching, angle bending, torsional rotation, and out-of-plane (improper) deformation. The nonbonded interactions are represented by a Lennard−Jones 9-6 and an exp-6 term for inter- as well as intramolecular van der Waals interactions. A Coulomb energy function is used to account for the electrostatic interactions. Within a crystal lattice the potential energy is translationally periodic over the unit cells. Using the unit vectors $\vec{a}$, $\vec{b}$, $\vec{c}$ and integers *i, j, k,* it is

$$U(\vec{r}) = U(\vec{r} + i\vec{a} + j\vec{b} + k\vec{c}). \quad (13)$$

In this work $\{i, j, k\} = \pm 1$ is used. This condition does not restrict the bonded contributions but the van der Waals interaction, the long-range electrostatic potentials, and the BPT calculation of the charges as well as chemical shift tensors. Nevertheless, the restriction to 27 unit cells ($3 \times 3 \times 3$) can be considered as a good first approximation for crystal structure simulations. Charges, energies, chemical shifts, and forces are calculated for the central cell. The outer cells are replicated in every step of the simulation. Starting from the Silk II fibroin model of Takahashi et al.,[22] a molecular dynamics simulation of the crystal was carried out with 2×10^4 time steps Δt of 0.5 fs at a slightly elevated temperature of 393 K. Every 100th time step a structure was saved. The resulting 200 snapshots were geometry optimized, and the chemical shift tensors were calculated and averaged. The simulation of the resulting NMR iso-aniso spectrum is shown in Figure 6. The intensities $I(\omega)$ of the tensor powder pattern spectra in the indirect ω_1 dimension are calculated according to the literature.[43] The resulting chemical shift tensor values are listed in Table 3. There is a

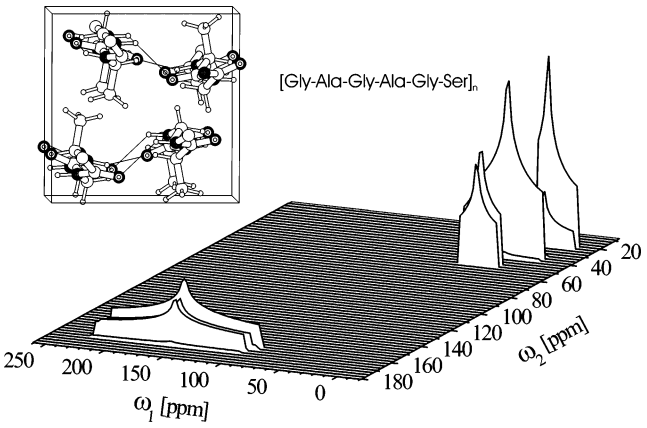

Figure 6. Simulated iso-aniso spectrum of *B. mori* silk fibroin according to the structural model of Takahashi et al.,[22] in which $(Gly\text{-}Ala)_n$ form two antipolar/antiparallel β-sheets with different orientations.

(41) Evans, D. J.; Morriss, G. P. *Statistical Mechanics of Nonequilibrium Liquids*; Academic Press: London, 1990.
(42) Möllhoff, M.; Sternberg, U. *J. Mol. Model.* **2001**, *7*, 90.
(43) Grant, D. M.; Harris, R. K. *Encycl. Nucl. Magn. Reson.* **1996**, *2*, 1298.

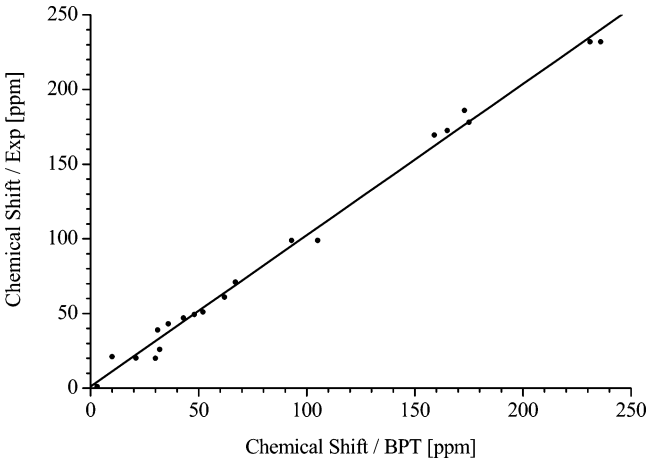

Figure 7. Correlation between the averaged BPT chemical shift tensor values and experimental results of the RAI sequence ($R = 0.997$, SD = 6.3 ppm). The standard deviations are 2 and 8 ppm for the experimental and theoretical values, respectively.

remarkably good correlation ($R = 0.997$) between the theoretical average tensor values and our experimental NMR data, as seen in Figure 7. Considering the deviations between our BPT calculations and the NMR experiment, it has to be kept in mind that all structures are produced by a molecular mechanics force field.

Discussion

In this work the RAI (recoupling of anisotropy information) pulse sequence has been introduced for measuring the chemical shift anisotropies with high resolution, by means of a 2D CP MAS iso-aniso experiment. This concept of recoupling the chemical shift powder pattern accounts for finite pulse lengths during $N = 3$ and 5 rotor cycles. It can be applied to spinning speeds up to 15 kHz as well as on samples with high or low abundance and high or low density nuclei. Overlapping CS tensor patterns are well resolved, as seen in Figure 5. The improved RAI experiment was first tested on polycrystalline amino acids (Gly, Ala, Ser) as model compounds, and its accuracy (2 ppm) was examined. Then, RAI was applied to the silk protein fibroin from *B. mori* (Cp-fraction with Silk II structure). For the first time, the complete sets of chemical shift anisotropy parameters for all ^{13}C sites on glycine, alanine, and serine in the native protein were obtained. The CS tensors are a rich source of structural information. In an NMR investigation of spider silk, van Beek et al.[44] used 2D NMR correlation spectroscopy (DOQSY) to investigate the distribution of dihedral angles in the polyalanine chains. To extract any bond or dihedral angles from these tensor correlation experiments, the carbon CS tensors including their orientation within the molecular frame must be known beforehand and the authors could only solve this problem using preliminary values from other investigations. Their alanine carbonyl principal values (246 ppm, 184 ppm, 89 ppm) are in good agreement with the poly-L-alanine data of Zhou et al.[29] (249 ppm, 178 ppm, 91 ppm), $^{13}C_1$-Ala silk fibroins from *B. mori* by Demura et al.[45] (242 ppm, 186 ppm, 96 ppm), and our experimental (232 ppm, 186 ppm, 99 ppm) and theoretical values (236 ppm, 173 ppm, 105 ppm). Differences may be attributed to the fact that poly-Ala in spider silk assumes a helical conformation, while $[Gly\text{-}Ala]_n$ in *B. mori* fibroin forms extended β-strands.

Having demonstrated the successful application of the RAI experiment the next step is to use the CS tensor data in direct NMR 3D structure refinements of macro molecules. One prerequisite of this task is the possibility to calculate accurate CS tensors for large molecular domains including lattice effects. Therefore, we performed chemical shift calculations for a central unit cell of silk fibroin, which included the interactions with 26 neighboring cells (see Table 3). The CS tensor values given in Table 3 are calculated from a structure that was obtained by geometry optimization of the silk II coordinates of the Takahashi model.[22] The crystal structure optimization for the central unit cell gave an energy minimum with coordinates that differed only 0.1 Å from the starting values. In this way we verified that (i) the Takahashi coordinates[22] represent a minimum with respect to our force field, (ii) that chemical shift tensors can be calculated precisely enough from force field structures, and (iii) that it makes sense to perform MD simulations including chemical shifts.

Because of the good correlation between the calculated CS tensors and the experimental values ($R = 0.997$) we can now produce reliable theoretical data concerning the orientation of all ^{13}C CS tensors for further tensor correlation measurements. Different authors[44,46−48] assumed that the most shielded axis of the ^{13}C carbonyl CS tensor is perpendicular to the carbonyl plane and that the intermediate shielded component should not deviate much (5°−13°) from the C═O bond direction. Analyzing the ^{15}N and ^{13}C powder patterns of isotope enriched small peptide models, Asakura et al.[49] found an angle of 0° between the δ_{22} principal tensor component and the C—N bond direction, which corresponds to an angle of about 30° with respect to the C═O bond. Single-crystal investigations[50] of different crystal forms of glycine-dipeptides revealed values between 5° and 13°, and an analysis of $^{15}N-^{13}C$ dipolar coupled powder patterns[51] of alanine-dipeptides gave 3.6°. In our calculation we obtained an angle of 31.2° for the glycine residue (see Figure 8) and 13.7° for alanine. Obviously the tensor orientation is highly susceptible to the molecular environment. Only the perpendicular orientation of the δ_{11} component to the carbonyl plane is conserved. Additionally, there is a tendency that the δ_{22} component of alanine is better aligned along the C═O bond direction than that of glycine. The exact tensor orientations, ranging in the case of alanine from 3.6° to 13.7° (our calculations), should have a considerable influence on the bond and dihedral angles when NMR tensor correlations are used to calculate molecular structures.

The next questions to be addressed by the MD simulation of the silk fibroin was whether internal motions change the tensors and to what extent the measured values are motional mean values. Therefore, 10 ps MD crystal simulations in 0.5 fs steps

(44) Van Beek, J. D.; Beaulieu, L.; Schäfer, H.; Demura M.; Asakura, T.; Meier, B. H. *Nature* **2000**, *405*, 1077.
(45) Demura, M.; Minami, M.; Asakura, T.; Cross, T. A. *J. Am. Chem. Soc.* **1998**, *120*, 1300.
(46) Oas, T. G.; Hartzell, C. J.; Dahlquist, F. W.; Drobny, G. P. *J. Am. Chem. Soc.* **1987**, *109*, 5962.
(47) Stark, R. E.; Jelinski, L. W.; Ruben, D. J.; Torchia, D. A.; Griffin, R. G. *J. Magn. Reson.* **1983**, *55*, 266.
(48) Separovic, F.; Smith, R.; Yannoni, C. S.; Cornell, B. A. *J. Am. Chem. Soc.* **1990**, *112*, 8324.
(49) Asakura, T.; Yamazaki, Y.; Seng, K. W.; Demura, M. *J. Mol. Struct.* **1998**, *446*, 179.
(50) Takeda, N.; Kuroki, S.; Kurosu, H.; Ando, I. *Biopolymers* **1999**, *50*, 61.
(51) Hartzell, C. J.; Whitfield, M.; Oas, T. G.; Drobny, G. P. *J. Am. Chem. Soc.* **1987**, *109*, 5966.

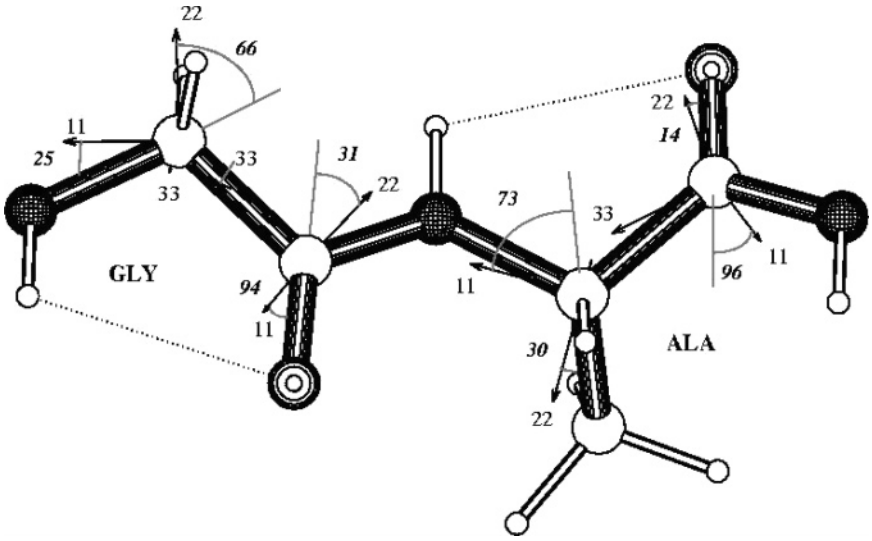

Figure 8. Glycine-alanine fragment of the silk fibroin polypeptide chain. The calculated chemical shift tensor orientations with respect to the molecular environment are shown. ($|\delta_{33} - \delta_{iso}| \geq |\delta_{11} - \delta_{iso}| \geq |\delta_{22} - \delta_{iso}|$).

were performed, and the tensors were averaged over 100 snapshot configurations. The correlation of the averaged values ($R = 0.997$, SD = 6.3) is better than the static values ($R = 0.991$, SD = 10.1 ppm), but significant changes of selected tensors are not observed. The calculated values support the Takahashi model,[22] but the existence of other models cannot be excluded. We performed our MD simulations at slightly elevated temperatures (393 K) to cover a larger region of the configuration space. Jumps into significantly different configurations were not observed in these MD runs.

Two newly developed methods have been thus presented here: the RAI experiment has been used to measure CS tensor data, and a procedure has been introduced to calculate these values under the influence of the crystal lattice. These methods were applied to silk, because fibrous proteins are of general interest due to their outstanding mechanical properties and because of their connection to diseases caused by amyloid fibrils. The ultimate aim of these investigations was crystal or molecular structure refinements using NMR chemical shifts. To take advantage of the wealth of information in CS tensor data, we first had to be sure that our NMR and MD methods could have been safely applied to proteins, which has been demonstrated here. The next step will be to proceed to 3D structure investigations of biomolecules using CS tensor data.

Acknowledgment. The authors thank Dr. K. Heinemann of the Thüringer Institut für Textil- und Kunststoff-Forschung e.V. for the silk sample and the DFG-CFN Karlsruhe for financial support and infrastructure.

Supporting Information Available: Data available in zip file. This material is available free of charge via the Internet at http://pubs.acs.org.

JA051730F